Journal of ELECTRICAL ENGINEERING, VOL 73(2022), NO5, 332–336

sciendo

PAPERS

Optimal design and low noise realization of digital differentiator

Om Prakash Goswami, Aasheesh Shukla*, Manish Kumar[1]

This manuscript presents a design of a differentiator in the digital domain with its low noise realization. It manifests the minimization of the L_1-error objective function by using a hybrid optimization technique consisting of the particle swarm and simulated annealing optimization algorithm. The obtained magnitude response provides a noteworthy approximation of the ideal differentiator with a minimal magnitude inaccuracy when compared with the existing designs. The realization structures are also investigated and compared in terms of the noise gain behavior.

K e y w o r d s: direct wave-form, hybrid optimization, L_1 error fitness function, Low noise design, realization

1 Introduction

Differentiators in digital domain are crucial in the variety of physical phenomena since most signal processing is done in the digital domain. It calculates the time rate of change of any applied real-time or measured excitation given to the system. Digital Differentiators have typically been understood in the engineering field as a linear system or filter with a predetermined frequency and time response. As opposed to analogue differentiators, which use resistors, inductors and capacitors to give rigidity in the configurations, digital differentiators use multipliers, adders and delays to provide flexibility. Due to its wide range of applications in fields like image processing, radar signalling, and biomedical engineering, the accurate approximation of digital differentiator has become increasingly compelling for researchers and designers in current years [1–3].

Literature shows that in recent years, various approaches based on mathematical formulations, fractional delays, and metaheuristic optimizations have been employed to design the different infinite impulse response (IIR) approximations of the ideal differentiator. Linear interpolation, Simpson integration, Newton-cotes integration, and segment rule are some mathematical frameworks that have been applied to approximate the digital differentiator [4–7]. Then, the utilization of fractional delays in place of integer delays has further improved the magnitude approximation [8]. Furthermore, some metaheuristic optimizing algorithms like simulated annealing (SA), multi-verse optimization (MVO), real-coded genetic algorithm (RCGA), bat algorithm (BA), and others has been applied to optimize the generalized transfer function of different order. They offer low absolute magnitude error in the approximation of the differentiator but with a higher order [9–15].

Another aspect of low complexity is its implementation in different realization structures. The most preferred realization structures comprise direct form-II (DF-II), cascade, parallel, and lattice forms of realizations. Each realization structure has its own merits and demerits. These structures may be coefficient sensitive, which produces a high quantization noise. An alternative realization to the conventional realizations must be investigated to provide low quantization noise [16].

In this work, an optimal design of low-order IIR digital differentiator is proposed. The design has been derived after optimizing the second-order transfer function in the L_1-sense error function. The obtained design approximates the ideal differentiator with the least absolute magnitude error in the region of interest. The realization structure of the proposed design has also been investigated to discuss low noise behavior.

2 Problem formulation and design

Mathematically, the ideal digital differentiator can be written as

$$H_{\mathrm{diff}}(\omega) = j\omega\,, \quad -\pi \le \omega \le \pi\,, \tag{1}$$

where ω is the angular frequency and $j = \sqrt{-1}$. It is recursively characterized and approximated by a N-order IIR digital system as [16]

$$y(n) = -\sum_{k=0}^{N-1} \alpha_k y(n-k) + \sum_{k=0}^{M-1} \beta_k x(n-k)\,, \tag{2}$$

where α_k and β_k are the coefficients of the digital system. The z-domain representation of the canonic transfer function of leads

$$H(z) = \frac{\sum_{k=0}^{M} \beta_k z^{-k}}{\sum_{k=0}^{N} \alpha_k z^{-k}}\,. \tag{3}$$

[1] Department of ECE, GLA University, Mathura, India, om9837@gmail.com, manish.kumar@gla.ac.in, *corresponding author: aasheesh.shukla@gla.ac.in,

https://doi.org/10.2478/jee-2022-0044, Print (till 2015) ISSN 1335-3632, On-line ISSN 1339-309X

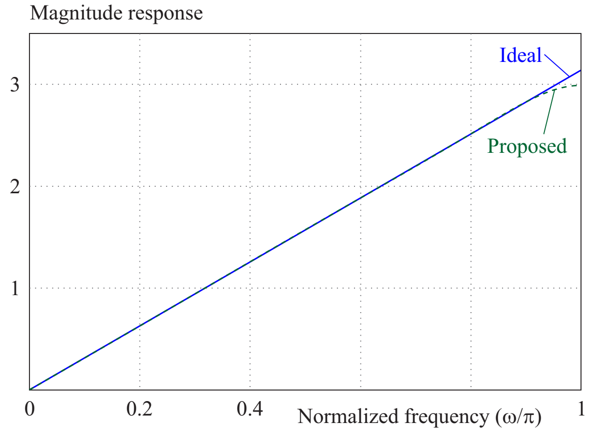

Fig. 1. Magnitude response of $H_{\text{diff}}(z)$ and $H_{\text{prop}}(z)$

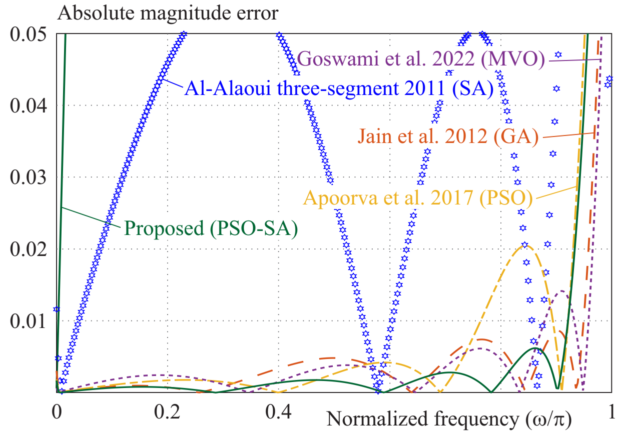

Fig. 2. AME comparisons

With $\alpha_0 = 1$, system function of the generalized second-order canonic digital differentiator can be written as

$$H(z) = k\frac{B_0z^2 + B_1z + B_2}{z^2 - A_1z - A_2}\,. \tag{4}$$

The generalized transfer function's five coefficients, $B0$, $B1$, $B2$, $A1$, and $A2$, as well as the constant multiplier k, can be optimized for the second-order digital differentiator to reduce the absolute error between the ideal and approximative magnitude response. The error function E can be defined as

$$\|E\| = \sum_{\omega} |(|H_{\text{diff}}(\omega)| - |H(z)_{z=e^{j\omega}}|)|\,, \tag{5}$$

where $\|\cdot\|$ provides norm of function. The L_1-norm based error objective function is utilized to optimize the transfer function's variables because at discontinuity points, it offers smooth response with reduced overshoot and ripples [13].

3 Hybrid optimization for the design of digital differentiator

This section gives a short description of the hybrid optimization consisting of particle swarm optimization (PSO) and simulated annealing optimization technique. To achieve the best results, the error objective function based on L_1-norm provided in (5) has been minimized and assessed at each iteration. PSO is a problem-independent stochastic search optimization technique, which is its fundamental advantage, but its stochastic character causes it to expose a lack of global searching capability at the end of a run. Whereas SA is a heuristic-based global search optimization technique which accepts both weaker and superior candidate solutions during the search process. Therefore, the integration of PSO with SA balances the required tradeoff between exploring and exploitation of the search spaces [7]. The metropolis criterion of choosing the solution can be written as

$$a(x) = \begin{cases} 1 & \text{if} \quad \delta E \le 0\,, \\ e^{-\delta E/T} & \text{if} \quad \delta E \ge 0\,, \end{cases} \tag{6}$$

where T denotes the system's current temperature and δE is the change in energy caused by a parameter perturbation. In order to verify the (6), a random number $\rho \in [0,1]$ is created, and its equality with $\rho \le a(x)$ is tested. Here, an appropriate cooling schedule based on adaptive simulated annealing (ASA) is presented to update the system's temperature [8]. Therefore, for k^{th} iteration the annealing schedule can be formulated as

$$T(K) = T(0)e^{Ck^{Q/D}}\,, \tag{7}$$

where $T(0)$ and D stand for the initial temperature, quenching factor, respectively, and D denotes the search space dimension. Finally, to save execution time and computational effort, the appropriate number of iteration and other control parameters have selected. In control parameters, with a population size of 150, the coefficient's lower and upper bounds are constrained to be between -1 and 1. The other parameters have been set as inertia weight $(\omega) = 0.9\,|\,0.4$, initial temperature $(T_0) = 50$, minimum temperature $(T_{\min}) = 10^{-10}$ and cooling schedule $(c = 0.01)$, $Q = 0.01$.

4 Analysis

4.1 Simulation analysis and the comparison with the existing second-order digital differentiator

The optimized values for B_0, B_1, B_2, A_1, A_2 and constant multiplier k are obtained as 0.754, 0.179, -1.698, 1.990, 0.178 and 1.289 respectively. The transfer function can be written as

$$H_{\text{prop}}(z) = 1.289\frac{0.754z^2 + 0.939z - 1.698}{z^2 + 1.990z + 0.178}\,. \tag{8}$$

The poles location of (8) are determined to be -1.8961 and -0.0941 in order to address stability concerns. Since the system is unstable due to the pole at $z = 1.896$, the pole reflection approach is employed to stabilize the system without compromising its magnitude response and associated magnitude errors [9]. Therefore, the suggested

Table 1. Statistical comparison

Technique	SAME $0 \leq \omega \leq 0.92\pi$	SAME $0 \leq \omega \leq \pi$
Al-Alaoui 2011 (SA), [10]	9.98	13.03
Jain et al. 2012 (GA), [11]	0.84	1.72
Apoorva et al. 2017 (PSO), [14]	1.21	3.08
Goswami et al. 2022 (MVO), [15]	0.86	1.60
Proposed (PSO-SA)	0.43	2.06

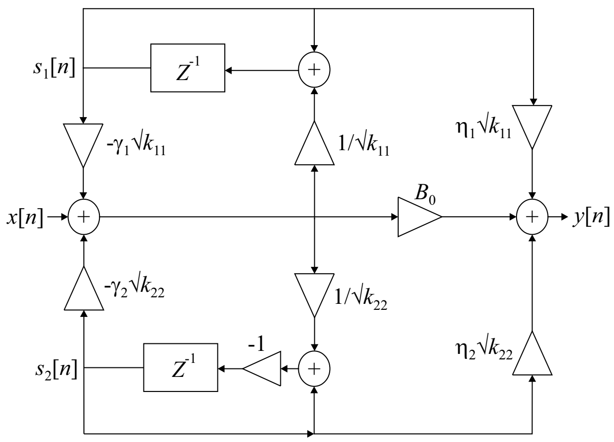

Fig. 3. Direct form-II realization

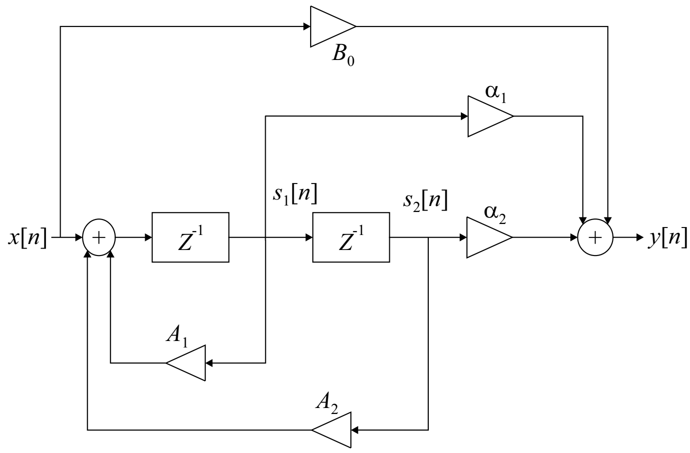

Fig. 4. Unscaled direct wave-form realization

second-order differentiator's transfer function can be rewritten as

$$H_{\mathrm{prop}}(z) = \left[1.289\frac{0.754z^2 + 0.939z - 1.698}{(z + 1.896)(z + 0.094)}\right]$$

$$= \left[1.289\frac{0.754z^2 + 0.9395z - 1.698}{(z + 1.896)(z + 0.094)}\right] \times \left[\frac{z + 1.896}{1.896z + 1}\right]$$

$$H_{\mathrm{prop}}(z) = \left[1.289\frac{0.754z^2 + 0.939z - 1.698}{1.896z^2 + 1.178z + 0.094}\right]. \qquad (9)$$

The magnitude response of the proposed design is plotted in Fig. 1, where it approximated the ideal response for almost the entire Nyquist region. The comparison of the absolute magnitude error of the proposed design and the existing design with the ideal response is plotted in Fig. 2.

Existing designs based on the optimization technique bestow the optimum correlation and provide the low magnitude error. The proposed designs confer the least magnitude error from 0.001π to 0.92π. The enlisted sum of absolute magnitude error (SAME) in Tab. 1 also confirms the eminence of the proposed design. The SAME of the proposed design is calculated as 0.428 for $0 \leq \omega \leq 0.92\pi$ which is the least among others. Therefore, the proposed designs perform better and outrange the other optimization-based designs.

4.2 Realization structures for the digital differentiator

The generalized transfer function of (4) can be rewritten as

$$H(z) = B_0 + \frac{\alpha_1 z + \alpha_2}{z^2 - A_1 z - A_2}\,, \qquad (10)$$

where $\alpha_1 = B_1 + A_1 B_0$ and $\alpha_2 = B_2 + A_2 B_0$ can be calculated from (9). The obtained transfer function has five degrees of freedom and can be implemented using direct form-II as shown in Fig. 3. It is the most widely used structure as it provides flexibility and simplicity. However, it is sensitive to the coefficient quantization and noise gain performances in fixed-point applications [5]. The optimal form and the normal form may be applied to mitigate the noise gain, but they utilize the extra degree of freedom to achieve it. Besides, they are not a straightforward implementation in terms of multiplier and coefficients. Therefore, another alternative direct waveform (DWF) structure can be used to realize the proposed design as it has a direct relationship between the transfer function's coefficients and DWF coefficients. Therefore, to acquire direct wave-form representation first (4) must converted into its appropriate representation of state-space followed by corroding similarity transformations [19].

In DWF realization, the proposed transfer function consisting five coefficients γ_1, γ_2, η_1, η_2, d with constant k can be obtained directly from direct form-II coefficients using relation as $\gamma_1 = 1/2(1 - A_1 - A_2)$, $\gamma_2 = 1/2(1 + A_1 - A_2)$ and $\eta_1 = 1/2(B_0 + B_1 + B_2)$, $\eta_2 = 1/2(B_0 - B_1 + B_2)$. The application of L_2 scaling makes this structure overflow stable, therefore in order to scale DWF structure two extra multiplier have been introduced as $1/\sqrt{K_{11}} = \sqrt{\gamma_1(2-\gamma_1-\gamma_2)}$ and $1/\sqrt{K_{22}} = \sqrt{\gamma_2(2-\gamma_1-\gamma_2)}$. Figure 4 depicts the scaled direct wave-form structure with their respective scaled coefficients [19].

4.3 Noise gain analysis

For calculating the noise power, the summation nodes quantizers at the output of the proposed digital differentiator structure must be analyzed. These quantizers provide the noise with the power of $q^2/12$ at the respective points. The output noise is calculated by the power gains, which require the observability matrix $W = \sum_{k=0}^{\infty}(CA^k)^t(CA^k)$. The principal diagonals provide the required power gain for calculating the noise gain. Therefore, the noise gain (G) is just the trace of this matrix $G = \mathrm{tr}(W)$. However, it results in is the unscaled noise, which raises the problem of the overflow of the states. Therefore, to prevent the overflow and improve the noise gain behavior, scaling must be done. It requires the controllability matrix K which can be defined recursively as $K = \sum_{k=0}^{\infty}(A^kB)(A^kB)^t$. The principal diagonal elements are the power gains from input to the states. Therefore the noise gains after scaling yields [20, 21]

$$G = K_{11}W_{11} + K_{22}W_{22}\,. \tag{11}$$

This work compares the realization perspective in terms of the conventional DF-II and the DWF structure.

4.3.1 Noise gain analysis for direct form-II structure

$$G_{\text{SDF-II}} = \frac{(1-A_2)^2\alpha_1^2 + (1-A_2)^2\alpha_2^2) + 2A_1(1-A_2)\alpha_1\alpha_2}{(1+A_2)^2(1-A_1-A_2)^2(1-A_1+A_2)^2}\,. \tag{12}$$

The incorporation of term B_0 leads the change the power gain which results in noise gain for DF-II

$$G_{\text{DF-II}} = G_{\text{SDF-II}} + \frac{B_0^2(1-A_2)}{(1+A_2)(1-A_1-A_2)(1-A_1+A_2)}\,. \tag{13}$$

Hence, the noise gain calculated for the proposed digital differentiator from the DF-II coefficients results in 5.885.

4.3.2 Noise gain analysis for direct wave-form structure

The noise gain of L_2-scaled DWF

$$G_w = K_{11w}W_{11w} + K_{22w}W_{22w}\,. \tag{14}$$

The controllability matrix (K_w), which proves to be diagonal, can be written as

$$\mathbf{K}_w = \frac{1}{4\gamma_1\gamma_2(2-\gamma_1-\gamma_2)}\begin{bmatrix}4\gamma_2 & 0\\ 0 & 4\gamma_1\end{bmatrix}. \tag{15}$$

The stability constraints are bounded by $\gamma_1, \gamma_2 \geq 0$, $2 - \gamma_1 - \gamma_2 \geq 0$. The observability matrix can be define as $W_w = T^t{}_w W T_w$, where W is the observability matrix of SDF-II. Calculating the diagonal entries of W_w and using diagonal entries of K_w with (14) yields the noise gain for DWF structures as [15]

$$G_{\text{SDF-II}} = \frac{(g_1\alpha_1^2 + g_2\alpha_2^2) + g_3\alpha_1\alpha_2}{(1+A_2)^2(1-A_1-A_2)^2(1-A_1+A_2)^2}\,, \tag{16}$$

where

$$g_1 = (1 + A_2^2)(1 - A_2)^2 - A_1^2 + A_1^2(1 + A_2)^2, \tag{17}$$

$$g_2 = 2(1 - A_2)^2 - A_1^2 + A_1^2(1 + A_2)^2, \tag{18}$$

$$g_3 = 2a(A_1 - A_2)^2 - A_1^2 + 2A_1(1 - A_2)(1 + A_2)^2. \tag{19}$$

From (9) and (16)-(19), The noise gain based in Fig. 4 of the proposed digital differentiator is calculated as 2.0679, which shows the improvement of $64.88\,\%$ compared to the direct form-II structure shown in Fig. 3. Therefore, it is observed that the DWF structure shows less noise gain than the DF-II structure for the proposed digital differentiator design.

5 Conclusion

This manuscript has presented an optimum design and low noise realization of the IIR digital differentiator. The design entails using the hybrid optimization method to optimize generalized second-order transfer function coefficients with an error objective function based on the L_1-norm. The design performs better than the current IIR differentiator designs in the region of interest, giving SAME 0.4281 and 2.0463 for $0 \leq \omega \leq 0.92\pi$ and $0 \leq \omega \leq \pi$, respectively. The investigation for the realization structures for the proposed design has also been discussed and DWF structure provides the improvement of 64.88% in noise gain as compared to the conventional direct-II from realization. Therefore, it has been concluded that the L_1-PSO-SA based digital differentiator design with its direct wave-form-based realization provides computational efficacy in real sense.

References

[1] P. Laguna, N. V. Thakor, P. Caminal, and R. Jane, "Low-pass differentiators for biological signals with known spectra: application to ECG signal processing", *IEEE Transactions on Biomedical Engineering*, no. 4, pp. 420-425, April 1990.

[2] A. Agrawal, V. Goyal, and P. Mishra, "A novel augmented fractional order fuzzy controller for enhanced robustness in nonlinear and uncertain systems with optimal actuator exertion", *Arabian Journal of Science and Engineering, Springer*, no. 10, pp. 10185-10204, 2021.

[3] M. A. Al-Alaoui, "Novel FIR approximations of IIR differentiators with applications to image edge detection", *18th IEEE International Conference on Electronics, Circuits, and Systems, Beirut*, 554-558, 2011.

[4] M. A. Al-Alaoui, "A class of second-order integrators and low-pass differentiators", *IEEE Transactions on Circuits and Systems I: Fundamental Theory and Applications*, no. 4, pp. 220 –223, 1995.

[5] N. Q. Ngo, "A new approach for the design of wideband digital integrator and differentiator", *IEEE Transactions on Circuits and Systems II: Express Briefs*, no. 9, pp. 936 –940, 2006,.

[6] P. Singh, V. Goyal, V. K. Deolia, and T. N. Sharma, "Sliding mode control of uncertain nonlinear discrete delayed time system using Chebyshev neural network", *Advances Computer and Computational Sciences, Advances Intelligent Systems and Computing, Springer*, vol. 553.

[7] C. Tseng, "Closed-form design of digital IIR integrators using numerical integration rules and fractional sample delays", *IEEE Transactions on Circuits and Systems I: Regular Papers*, no. 3, pp. 643 –655, 2007.

[8] S. Pei and H. Hsu, "Fractional bilinear transform for analog-to-digital conversion", *IEEE Transactions on Signal Processing*, no. 5, pp. 2122-2127, May 2008.

[9] M. A. Al-Alaoui, "Class of digital integrators and differentiators", *IET Signal processing*, no. 2, pp. 251-260, https://doi.org/10.1049/ietspr.2010.0107, 2011.

[10] M. Jain, M. Gupta, and N. Jain, "Linear phase second order recursive digital integrators and differentiators", *Radio Engineering Journal*, no. 2, pp. 712–717, 2012.

[11] N. Bansal, V. K. Deolia, A. Bansal, and P. Pathak, "Comparative analysis of LSB, DCT and DWT for Digital Watermarking", *2nd International Conference on Computing for Sustainable Global Development*, pp. 40-45, 2015.

[12] M. A. Al-Alaoui, "A class of second-order integrators and low-pass differentiators", *IEEE Transactions on Circuits and Systems I: Fundamental Theory and Applications*, no. 4, pp. 220 –223, 1995.

[13] A. Aggarwal, T. K. Rawat, and D. K. Upadhyay, "Optimal design of L 1-norm based IIR digital differentiators and integrators using the bat algorithm", *IET Signal Processing*, no. 1, pp. 26-35, 2017.

[14] A. Sharma, R. Chaturvedi, and A. Bhargava, "A novel opposition based improved firefly algorithm for multilevel image segmentation", *Multimed. Tools Appl*, pp. 15521–15544 2022.

[15] O. P. Goswami, T. K. Rawat, and D. K. Upadhyay, "L1-norm -based optimal design of digital differentiator using multiverse optimization", *Circuits, Systems, and Signal Processing*, 2022.

[16] A. V. Oppenheim, R. W. Schafer, and J. R. Buck, *Discrete-Time Signal Processing*, 1999.

[17] S. Dhabal and P. Venkateswaran, "Two-dimensional IIR filter design using simulated annealing-based particle swarm optimization", *Journal of Optimization*, 2014, Article ID 239721, 2014.

[18] F. Zhao, Q. Zhang, D. Yu, X. Chen, and Y. Yang, "A hybrid algorithm based on PSO and simulated annealing and its applications for partner selection in virtual enterprise", *Proceedings of the International Conference on Advances Intelligent Computing*, 380 –389, Springer, 2005.

[19] J. H. F. Ritzerfeld, "The direct waveform digital filter structure: an easy alternative for the direct form", *Proceedings of the 15th ProRISC, Annual Workshop on Circuits, Systems and Signal Processing*, pp. 133–137.

[20] L. Sajewski, "Positive minimal realization of continuous-discrete linear systems with all-pole and all-zero transfer function", *Acta Mechanica et Automatica*, no. 1, pp. 42–47, 2014.

[21] J. H. F. Ritzerfeld, "Noise gain expressions for low noise second-order digital filter structures ", *IEEE Transactions on Circuits and Systems II: Express Briefs*, vol. 52, no. 4, pp. 223–227, 2005.

Received 12 September 2022